Catalysis Letters Vol. 112, Nos. 3–4, December 2006 (© 2006)
DOI: 10.1007/s10562-006-0205-9

Graphitic spherical carbon as a support for a PtRu-alloy catalyst in the methanol electro-oxidation

Pil Kim,[a] Ji Bong Joo,[b] Wooyoung Kim,[b] Jongsik Kim,[b] In Kyu Song,[b] and Jongheop Yi[b,*]

[a]*School of Environmental and Chemical Engineering, Chonbuk National University, Chonbuk, Jeonju, 561–756, South Korea*
[b]*School of Chemical and Biological Engineering, Institute of Chemical Processes, Seoul National University, Shinlim-dong, Kwanak-ku, Seoul, 151–744, Korea*

Received 28 June 2006; accepted 18 October 2006

Spherical carbons were prepared using sucrose as a carbon precursor via hydrothermal method for use as supports for PtRu-alloy catalysts in the methanol electro-oxidation. Spherical carbon particles with an average diameter of 1μm (SC-1) were prepared under static condition (without stirring), while spherical carbon materials with a diameter of 500–600 nm (SC-2) were obtained under dynamic condition (with stirring). A graphitic spherical carbon material (SC-g) was successfully prepared by the addition of Fe salt under dynamic condition. It was revealed that the catalytic action of Fe species during the hydrothermal process was essential for the formation of a graphitic structure of SC-g. The surface areas were found to be 112, 383, and 252 m^2/g for SC-1, SC-2, and SC-g, respectively. PtRu nanoparticles were then supported on the spherical carbons by a $NaBH_4$-reduction method for use in the methanol electro-oxidation. The average metal particle sizes were 3.5, 2.6, and 2.7 nm for PtRu/SC-1, PtRu/SC-2, and PtRu/SC-g, respectively. The PtRu/SC-1 and PtRu/SC-2 showed a lower catalytic performance in the methanol electro-oxidation than the PtRu/Vulcan. However, the PtRu/SC-g exhibited a higher catalytic performance than the PtRu/Vulcan. It is believed that the high graphitic nature of SC-g was responsible for the enhanced catalytic performance of PtRu/SC-g.

KEY WORDS: spherical carbon; carbon precursor; hydrothermal method; graphitic carbon; methanol electro-oxidation.

1. Introduction

Direct methanol fuel cells (DMFC) are considered to be an alternative power source for portable electronic devices because of high power density and low operating temperature [1–3]. For the successful commercialization of DMFC, however, substantial improvements should be achieved in both constituent materials and operating processes. The electrode catalyst, a key component in DMFC, has attracted considerable attention to improve the performance of unit cell and cell stack. Many efforts have been made to prepare the highly active electrode catalyst in the methanol electro-oxidation [4–6]. Because large amounts of electrode catalyst are needed to obtain a desired power density in DMFC, an enhancement in catalyst utilization is essential for the successful commercialization of DMFC. To increase the catalyst utilization, electrode catalysts have been prepared in the form of nanoparticles supported on conductive carbon materials.

It is well known that the catalytic performance in DMFC is influenced by the physicochemical properties of the support [7–10]. A PtRu-alloy catalyst supported on graphite nanofibers was found to show a high catalytic activity in the methanol electro-oxidation, as a result of the enhanced electronic conductivity and the well-ordered graphitic structure of graphite nanofibers [11]. It was also reported that the strong interaction between active metal and graphitic carbon nanocoil had a beneficial effect on the methanol electro-oxidation [12, 13].

Many types of carbon precursors have been used in the preparation of carbon supports [14–18]. Among the carbon precursors, sucrose has many advantages in terms of non-toxicity and availability. However, it is known that carbon materials prepared using sucrose as a precursor usually retain an amorphous structure unless a harsh pyrolysis condition or an additional graphitization process is employed [18].

In this work, we prepared a graphitic spherical carbon using sucrose as a carbon precursor via hydrothermal method at a mild pyrolysis temperature. The prepared graphitic spherical carbon was used as a support for a PtRu-alloy catalyst in the methanol electro-oxidation. The catalytic performance of PtRu-alloy catalyst supported on carbon material was compared with that of PtRu/Vulcan catalyst.

2. Experimental

2.1. Preparation of spherical carbon

Amorphous spherical carbons (SC-1 and SC-2) and graphitic spherical carbon (SC-g) were prepared by a hydrothermal method. Sucrose (Aldrich) was dissolved

*To whom correspondence should be addressed.
E-mail: jyi@snu.ac.kr

in de-ionized water, and then the solution was charged into a Teflon-coated stainless steel autoclave. For the preparation of SC-g, a catalyst ($FeNO_3{\cdot}6H_2O$, Aldrich) was added into the precursor solution (molar ratio of sucrose:$FeNO_3{\cdot}6H_2O$ = 3:1). The autoclave was placed in a convection oven, and the mixture was hydrothermally treated with 350 rpm (SC-2 and SC-g) or without stirring (SC-1) at 190 °C for 7 h. After cooling the autoclave to room temperature, the black precipitate was filtered and dried. The black precipitate was finally pyrolysed at 900 °C to yield the spherical carbon. The Fe species in the SC-g were removed using HNO_3 solution. FE-SEM-EDX (Jeol JSM-6700F) analysis revealed that no iron was detected in the final SC-g sample, indicating the complete removal of Fe species from the SC-g. Surface morphologies of the prepared carbon materials were examined by FE-SEM analyses.

2.2. Preparation and characterization of supported PtRu-alloy catalyst

Carbon-supported PtRu-alloy catalysts were prepared by a $NaBH_4$-reduction method [12, 13]. Metal salts, $H_2PtCl_6{\cdot}xH_2O$ (Acros) and $RuCl_3{\cdot}xH_2O$ (Acros), were dissolved in de-ionized water (the ratio of Pt:Ru was fixed at 50 wt%:50 wt%), and then the solution was added into an aqueous solution containing carbon support. Aqueous $NaBH_4$ solution was added dropwise into the resulting mixture at 4 °C for the complete reduction of metal species. The carbon-supported PtRu-alloy catalysts were obtained by filtration and subsequent washing with de-ionized water, followed by drying at 120 °C overnight. For the purpose of comparison of catalytic performance, a PtRu catalyst supported on Vulcan XC-72 (Cabot, BET surface area of 230 m^2/g) was prepared by the same method.

X-ray diffraction (XRD, MAC/Science M18XHF-SRA) measurements were carried out in order to investigate the crystalline phases of carbon supports and supported PtRu-alloy catalysts. The lattice of carbon support and the location of PtRu-alloy particles on the carbon support were examined by transmission electron microscopy (TEM, Jeol JXA-8900R and HR-TEM, Joel 3300) using an ultrasonically dispersed catalyst sample (in a mixed solution of ethanol and distilled water) deposited on a carbon grid.

2.3. Methanol electro-oxidation

Methanol electro-oxidation was carried out in a conventional three-electrode system equipped with saturated calomel (reference electrode) and platinum gauze (counter electrode). The working electrode was prepared by coating a small amount of catalyst ink on disk-type graphite. Prior to the coating with the catalyst ink, the graphite surface was polished with alumina paste and washed with de-ionized water. Cyclic voltammograms were obtained at room temperature in 0.5 M H_2SO_4 solution containing 2 M CH_3OH with a scan rate of 10 mV/s (Potentiostat/Galvanostat EG & G 263A).

3. Results and discussion

3.1. Characterization of spherical carbon

Spherical carbon with an average size of 1μm was previously prepared by a hydrothermal method, in which an aqueous solution of sucrose was polymerized under static condition (without stirring) [19]. In this work, a similar result was observed for SC-1 sample (figure 1a) that was prepared under static condition. Spherical carbon with a particle size of 500–600 nm (SC-2) was also successfully prepared under dynamic condition (with stirring), as shown in figure 1b. On the other hand, SC-g sample was found to have a slightly irregular shape with a somewhat broad particle size distribution (figure 1c). This suggests that the growth mechanism of carbon particles derived from glucose followed the LaMer model, in which carbon nuclei are formed during the hydrothermal treatment and grow uniformly by the diffusion of solutes toward the surface of the particles [20]. This mechanism seems to hold for SC-1 and SC-2 samples. In the case of SC-g, however, a modified growth model should be considered due to the catalytic action of Fe species. Although the detailed mechanism for the growth of SC-g particles has not been fully understood, it is likely that the catalytic action of Fe species was involved in both polymerization and carbonization, resulting in somewhat irregular shaped carbon particles (figure 1c). The BET surface areas were determined to be 112, 383, and 252 m^2/g for SC-1, SC-2, and SC-g samples, respectively.

Figure 2 shows the XRD patterns of SC-1 and SC-g samples. SC-1 showed an amorphous nature, a typical feature of carbon material prepared using sucrose. XRD pattern of SC-2 was almost identical to that of SC-1, also indicating the amorphous nature of SC-2. However, SC-g sample showed the characteristic diffraction peaks for (002), (100), and (004) planes. The crystalline size measured perpendicular to the basal plane and the d_{002}-spacing for SC-g sample were found to be 4.4 nm and 3.41 Å, respectively. In particular, the degree of graphitization, which was obtained by applying the equation of 0.344-d_{002}/0.0086 [21], was determined to be 0.35, suggesting a highly graphitic structure of SC-g sample.

The graphitic nature of SC-g was further confirmed by Raman spectroscopy measurements as shown in figure 3. For the comparison purpose, Raman spectra of multi-wall carbon nanotube (MWCNT, IlJin Nanotek) and Vulcan XC-72 (Cabot) were also measured. All the carbon materials exhibited two distinct bands appearing at around 1350 cm^{-1} (D-band) and 1580 cm^{-1} (G-band). The D-band is closely related to the disorder-induced scattering resulting from the imperfections or the loss of hexagonal symmetry of the

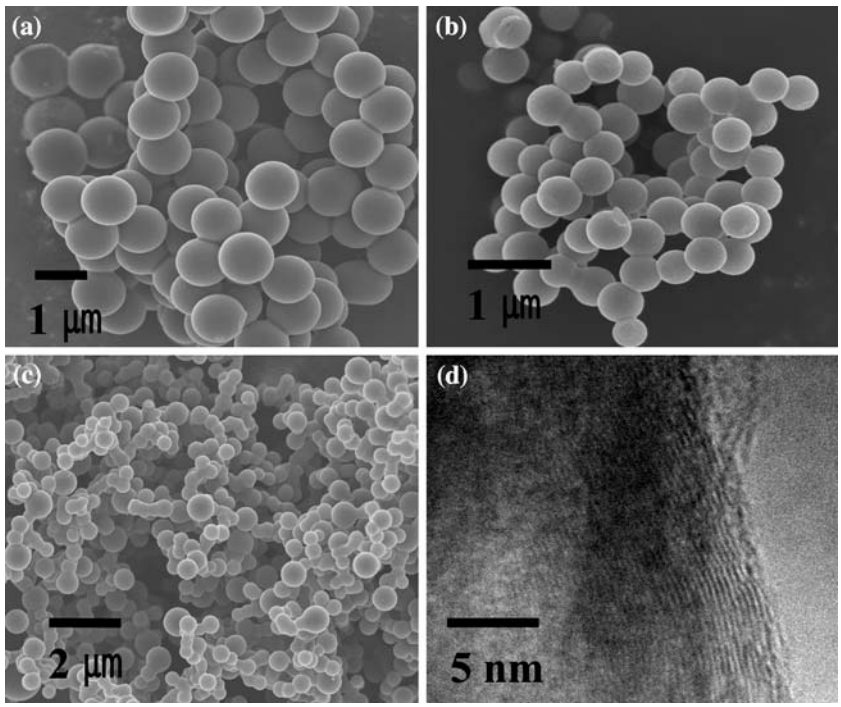

Figure 1. FE-SEM images of (a) SC-1, (b) SC-2, (c) SC-g, and HR-TEM image of (d) SC-g.

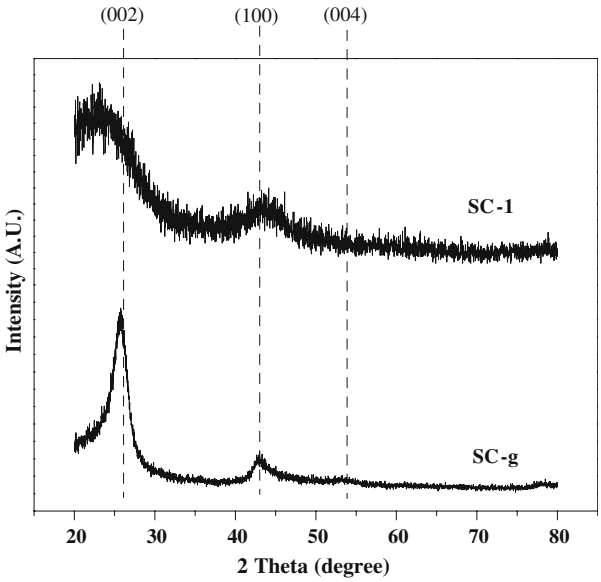

Figure 2. XRD patterns of SC-1 and SC-g.

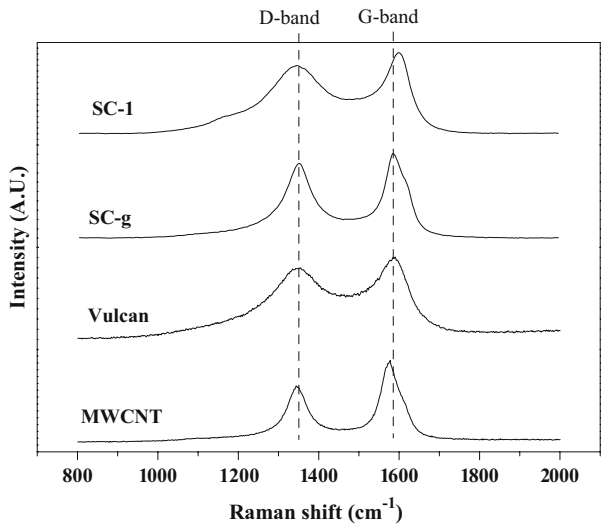

Figure 3. Raman spectra of carbon samples.

graphite structure; this band is not observed in perfect graphite [21]. On the other hand, the G-band is known to appear in both amorphous carbon and graphite. Therefore, the area ratio between the two bands (A_D/A_G) can be used as an index for the degree of graphitization [21, 22]. The results showed that the A_D/A_G value of SC-1 (2.02) was the largest among the carbon materials, indicating the lowest graphitization of SC-1. It should be noted that the A_D/A_G value of SC-g (1.08) was smaller than that of Vulcan carbon (1.65). Furthermore, a similar value of A_D/A_G between SC-g (1.08) and MWCNT (1.04) demonstrates that the SC-g retained comparable graphitic characteristics to the MWCNT. The HR-TEM image showing the edge of SC-g sample (figure 1d) revealed that the SC-g sample retained concentric graphene layers that were not observed in the SC-1 and SC-2 samples, also supporting the graphitic nature of SC-g.

It is noteworthy that the graphitic spherical carbon was obtained at a mild pyrolysis temperature (900 °C) in this work. In order to investigate the effect of synthesis parameters on the development of graphitic structure,

we attempted to prepare a carbon material without hydrothermal treatment. For this purpose, sucrose was dissolved in an aqueous solution of Fe precursor, followed by polymerization using aqueous solution of H_2SO_4 (denoted as C–H_2SO_4). The pyrolysis and the etching of Fe species were conducted at the same conditions as were employed for SC-g. The C–H_2SO_4 showed no characteristic XRD pattern as observed for the SC-1 sample, indicating the amorphous nature of C–H_2SO_4. This means that the hydrothermal treatment together with the catalytic action of Fe species were essential for the formation of a graphitic structure of SC-g. The aromatization of polymers derived from sucrose occurs during the hydrothermal treatment [19, 20]. In the case of SC-g, it is believed that both the polymerization of sucrose and the subsequent aromatization favorably proceeded by the catalytic action of Fe species, resulting in the development of aromatic polymer on the surface of Fe oxide. It has been reported that the graphitization of carbon is accelerated in the presence of catalysts such as metal and metal oxide [21]. Although the C–H_2SO_4 was prepared in the presence of Fe salt, a highly graphitized structure was not developed in this carbon material because no process to enhance aromatization was employed.

3.2. Characterization of supported PtRu-alloy catalyst

Figure 4 shows the XRD patterns of carbon-supported PtRu-alloy catalysts. The characteristic peaks for a face centered cubic phase (fcc) were clearly observed in all the catalysts. However, no peaks related to Ru or Ru-rich hexagonal closed packed phase (hcp) were observed. In particular, the characteristic peaks for pure Pt component, which are known to appear at 39.76° for Pt (111) and 64.47° for Pt (220), shifted to higher angles in the carbon-supported PtRu-alloy catalysts,

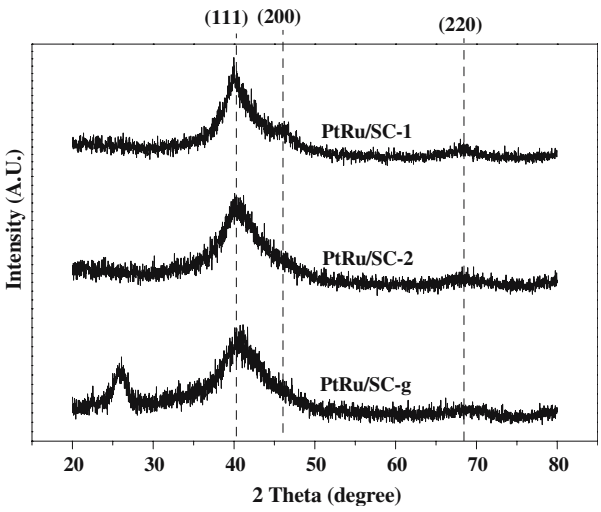

Figure 4. XRD patterns of carbon-supported PtRu-alloy catalysts.

indicating the lattice contraction as a result of PtRu-alloyM formation [23–25]. These results imply that the fcc structure of PtRu-alloy was dominant in the carbon-supported catalysts. By applying Scherrer's equation, the average metal particles sizes were measured to be 3.5, 2.6, and 2.7 nm for PtRu/SC-1, PtRu/SC-2, and PtRu/SC-g, respectively. Large metal particles were formed in the PtRu/SC-1 catalyst due to the small surface area of SC-1 support. The PtRu loading on the supported catalysts was 60 wt% in all cases.

Figure 5 shows the TEM images of carbon-supported PtRu-alloy catalysts. Fine metal particles with some agglomerate were deposited on the carbon supports. It should be noted that the formation of agglomerate was more intensive on the carbon support with low surface area (SC-1) than that with high surface area (SC-2 and SC-g), in good agreement with the XRD results (figure 4).

3.3. Catalytic performance in the methanol electro-oxidation

Methanol electro-oxidation was carried out in order to investigate the catalytic performance of the prepared catalysts. As shown in figure 6, all the catalysts exhibited a typical methanol-oxidation current behavior of a PtRu-alloy catalyst [26]. Compared to the conventional Pt/C catalyst, the PtRu-alloy catalysts showed a lower onset voltage in the methanol electro-oxidation, resulting from the bifunctional mechanism of PtRu-alloy catalyst (these are not shown here) [26–28]. All the supported PtRu catalysts tested in this work showed anodic peak current at 0.45–0.5 V, which was attributed to the methanol electro-oxidation. The catalytic performance of the prepared catalysts in the methanol electro-oxidation was evaluated by comparing their anodic peak currents. As shown in figure 6, the PtRu/SC-1 and PtRu/SC-2 showed a lower catalytic performance than the PtRu/Vulcan. The peak current densities were 9.9, 12.8, and 16.4 mA/cm^2 for PtRu/SC-1, PtRu/SC-2, and PtRu/Vulcan catalysts, respectively. However, the PtRu/SC-g exhibited 1.3 times higher catalytic performance than the PtRu/Vulcan at 0.5 V. It can be summarized that the PtRu/SC-g catalyst showed the highest catalytic performance among the catalysts tested in this work. The PtRu/SC-2 catalyst showed a higher catalytic performance than the PtRu/SC-1 due to the high metal dispersion of PtRu/SC-2 catalyst.

Carbon materials with a graphitic structure have been used as catalyst supports in low temperature fuel cells, and the unexpected enhancement in catalytic performance has frequently been observed [11–13, 29–31]. Although a detailed explanation for the enhanced catalytic performance was not provided, it is believed that the unique electronic property and the crystallographic orientation of graphitic carbon had a positive effect on the catalytic performance. Therefore, it is concluded

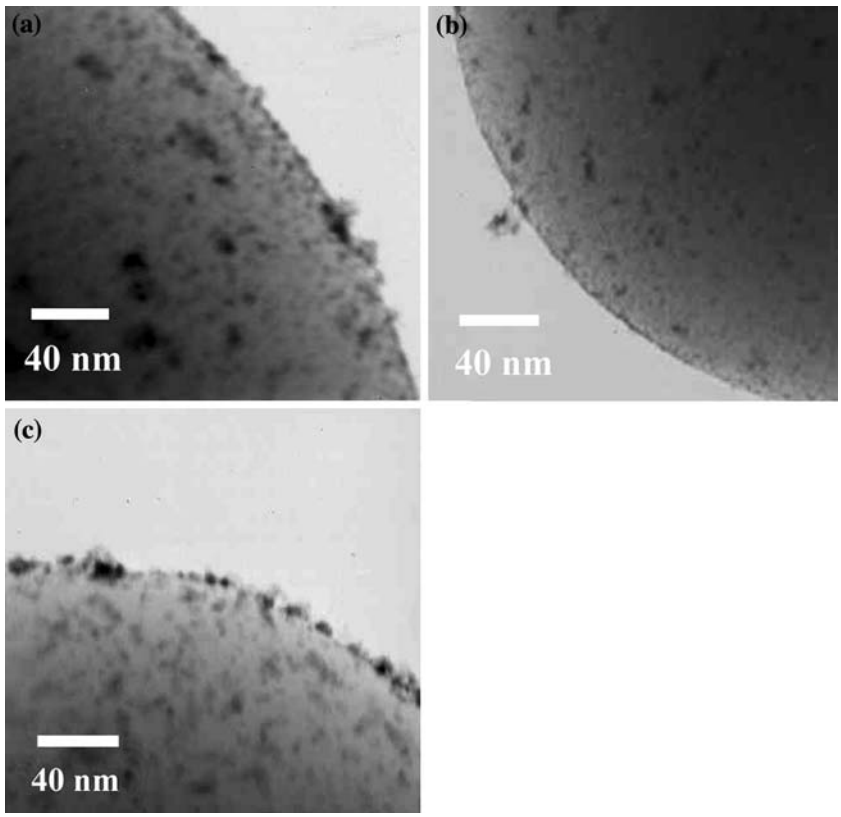

Figure 5. TEM images of (a) PtRu/SC-1, (b) PtRu/SC-2, and (c) PtRu/SC-g.

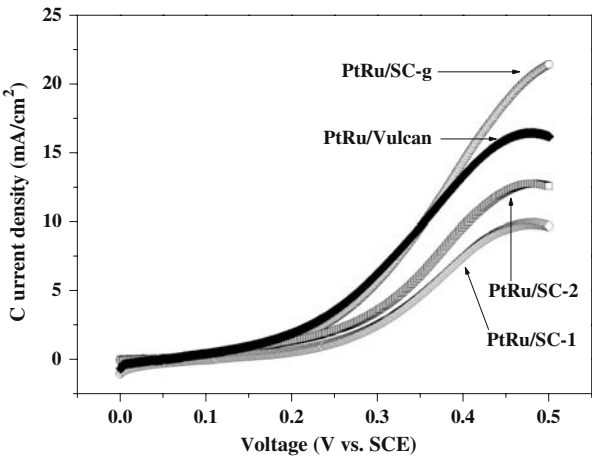

Figure 6. Cyclic voltammograms on carbon-supported PtRu-alloy catalysts (60 wt% loading) in 0.5 M H_2SO_4 containing 2 M CH_3OH (scan rate = 10 mV/s).

that the graphitic structure of SC-g had a positive effect on the catalytic function of PtRu/SC-g, resulting in the highest catalytic performance of PtRu/SC-g in the methanol electro-oxidation. It is also inferred that the PtRu/Vulcan showed a better catalytic performance than the PtRu/SC-2 due to the high graphitic nature of Vulcan.

4. Conclusions

Spherical carbons were prepared using sucrose as a carbon precursor via hydrothermal method for use as supports for PtRu-alloy catalysts in the methanol electro-oxidation. Spherical carbon with an average diameter of 1μm (SC-1) was prepared under static condition (without stirring), while spherical carbon material with diameter of 500–600 nm (SC-2) was obtained under dynamic condition (with stirring). In particular, a spherical carbon material with graphitic characteristics (SC-g) was produced by the addition of Fe salt under dynamic condition. It was found that both the hydrothermal treatment and the catalytic action of Fe were essential for the formation of a graphitic structure of SC-g. In the methanol electro-oxidation, the PtRu/SC-g exhibited the highest catalytic performance among the catalysts tested in this work. The catalytic performance was decreased in the order of PtRu/SC-g > PtRu/Vulcan > PtRu/SC-2 > PtRu/SC-1. It is concluded that the high graphitic nature of SC-g was responsible for the enhanced catalytic performance of PtRu/SC-g.

Acknowledgments

We are grateful to the Eco-Technopia-21 project of Ministry of Environment, Korea, and Hyundai-Kia Next Generation Vehicle Research Center for financial

support. This research was conducted through the Engineering Research Institute (ERI) at Seoul National University, Korea.

References

[1] M.S. Wilson and S. Gottesfeld, J. Appl. Electrochem. 22 (1992) 1.
[2] S. Surampudi, S.R. Narayanan, E. Vamos, H. Frank, G. Halpert, A. Laconti and G.A. Olah, J. Power Sources 47 (1994) 377.
[3] X. Ren, M.S. Wilson and S. Gottesfeld, J. Electrochem. Soc. 143 (1996) L12.
[4] J.Y. Kim, Z.G. Yang, C.C. Chang, T.I. Valdez, S.R. Narayanan and P.N. Kumta, J. Electrochem. Soc. 150 (2003) A1421.
[5] S.A. Lee, K.W. Park, J.H. Choi, B.K. Kwon and Y.-E. Sung, J. Electrochem. Soc. 149 (2002) A1299.
[6] T. Okada, Y. Suzuki, T. Hirose, T. Toda and T. Ozawa, Chem. Comm. (2001) 2492.
[7] M. Nurunnabi, B. Li, K. Kunimori, K. Suzuki, K. Fujimoto and K. Tomishige, Catal. Lett. 103 (2005) 277.
[8] X. Dong, H.-B. Zhang, G.-D. Lin, Y.-Z. Yuan and K.R. Tsai, Catal. Lett. 85 (2003) 237.
[9] R. Vieira, P. Bernhardt, M.-J. Ledoux and C.P. Huu, Catal. Lett. 99 (2005) 177.
[10] Y. Yazawa, N. Kagi, S. Komai, A. Satsuma, Y. Murakami and T. Hattori, Catal. Lett. 72 (2001) 157.
[11] C.A. Bessel, K. Laubernds, N.M. Rodriguez and R.T.K. Baker, J. Phys. Chem. B105 (2001) 8097.
[12] K.W. Park, Y.-E. Sung, S. Han, Y. Yun and T. Hyeon, J. Phys. Chem. B108 (2004) 939.
[13] T. Hyeon, S. Han, Y.-E. Sung, K.W. Park and Y.-W. Kim, Angew. Chem. Int. Ed. 42 (2003) 4352.
[14] M.S. Strano and H.C. Foley, Catal. Lett. 74 (2001) 177.
[15] F. Li, J. Zou and G. Yuan, Catal. Lett. 89 (2003) 115.
[16] F. Su, J. Zeng, Y. Yu, L. Lv, J.Y. Lee and X. Zhao, Carbon 43 (2005) 2366.
[17] Y. Xia and R. Mokaya, Adv. Mater. 16 (2004) 1553.
[18] T.W. Kim, I.W. Park and R. Ryoo, Angew. Chem. Int. Ed. 42 (2003) 4375.
[19] Q. Wang, H. Li, L. Chen and X. Huang, Carbon 39 (2001) 2211.
[20] X. Sun and Y. Li, Angew. Chem. Int. Ed. 43 (2004) 597.
[21] F.J. Maldonado, C. Moreno, J. Rivera, Y. Hanzawa and Y. Yamada, Langmuir 16 (2000) 4367.
[22] J. Jang and H. Yoon, Adv. Mater. 15 (2003) 2088.
[23] G.S. Chai, S.B. Yoon, J.-S. Yu, J.-H. Choi and Y.-E. Sung, J. Phys. Chem. B 108 (2004) 7074.
[24] C. Bock, C. Paquet, M. Couillard, G.A. Botton and B.R. MacDougall, J. Am. Chem. Soc. 126 (2004) 8028.
[25] G.G. Park, T.H. Yang, Y.G. Yoon, W.Y. Lee and C.S. Kim, Int. J. Hydro. Ener. 28 (2003) 645.
[26] Z. Liu, X.Y. Ling, X. Su and J.Y. Lee, J. Phys. Chem. B 108 (2004) 8234.
[27] A.S. Arico, S. Srinivasan and V. Antonucci, Fuel Cells 1 (2001) 133.
[28] G.A. Camara, R.B. de Lima and T. Iwasita, Electrochem. Comm. 6 (2004) 812.
[29] Z. He, J. Chen, D. Liu, H. Tang, W. Deng and Y. Kuang, Mater. Chem. Phys. 85 (2004) 396.
[30] T. Matsumoto, T. Komatsu, K. Arai, T. Yamazaki, M. Kijima, H. Shimizu, Y. Takasawa and J. Nakamura, Chem. Comm. 840 (2004).
[31] Z. Liu, X. Lin, J.Y. Lee, W. Zhang, M. Han and L.M. Gan, Langmuir 18 (2002) 4054.